ORIGINAL ARTICLE

Discrimination of earthquakes and quarry blasts in the eastern Black Sea region of Turkey

Şeyda Yılmaz · Yusuf Bayrak · Hakan Çınar

Abstract In recent years, a large number of quarry blasts have been detonated in the eastern Black Sea region. When these blasts are recorded by seismic stations, they contaminate the regional earthquake catalog. It is necessary to discriminate quarry blast records from the earthquake catalogs in order to determine the real seismicity of the region. Earthquakes and quarry blasts can be separated through different methods. These methods should be applied concurrently in order to safely distinguish these events. In this study, we discriminated quarry blasts from earthquakes in the eastern Black Sea region of Turkey. We used 186 seismic events recorded by the Karadeniz Technical University and Bogaziçi University Kandilli Observatory Earthquake Research Institute stations which are Trabzon, Espiye, Pazar, Borçka, Aydıntepe, and Gümüşhane between years of 2002 and 2010. For the discrimination of quarry blasts from earthquakes, we used both, statistical methods (calculation of the maximum ratio of S to P waves (S/P), complexity (C)) and spectral methods (spectrogram calculation). These methods included measuring the maximum amplitude S/P, C, spectral ratio, and time-frequency analysis. We especially relied on two-dimensional time-frequency analysis methods to discriminate quarry blasts from earthquakes in Turkey. As a result of this study, 68 % of the examined seismic events were determined to be quarry blasts and 32 % to be earthquakes. The earthquakes occurring on land are related to small faults and the blasts are concentrated in large quarries. Nearly 40 % of the earthquakes occurred in the Black Sea, most of them are related to the Black Sea thrust belt, where the largest earthquake was observed in the time period studied. The areas with the largest earthquake potential in the eastern Black Sea region are in the sea.

Keywords The eastern Black Sea · Earthquakes · Quarry blasts · Time-frequency analysis

1 Introduction

The eastern Black Sea region is related to the Eastern Pontides, known as the eastern Black Sea mountain belt. This belt takes part of the Alpine Himalayan orogen and elongates for about 600 km from Samsun in the W to Hopa in the E. The N-S extension from Trabzon (N) to Erzincan (S) amounts to approximately 125 km. Active deformation zones in the eastern Pontides create three different seismic belts from south to north (Bektaş et al. 1995; Eyüboğlu et al. 2007). These belts represent (1) a southern seismic zone

Ş. Yılmaz · Y. Bayrak (✉) · H. Çınar
Department of Geophysics, Karadeniz Technical University, Trabzon, Turkey
e-mail: bayrak@ktu.edu.tr

Ş. Yılmaz
e-mail: seydayilmaz@ktu.edu.tr

H. Çınar
e-mail: cinar@ktu.edu.tr

covering the North Anatolian Fault, the North East Anatolian Fault, and the region from Erzincan to Erzurum; (2) a middle seismic zone related to the eastern Black Sea region and coastal region; (3) a northern seismic zone covering the Black Sea. Figure 1 shows the generalized tectonic and geologic map showing these main zones and lithological units of the eastern Pontides. Chekunov et al. (1994) report that the seismic activity, the focal depths and the magnitudes increase from N to S depending on the thickness and properties of the crust. Seismic activity has been observed along fault lines such as the Bayburt–Gümüşhane–Espiye Fault line and the Alucra–Torul–Trabzon Fault line (Bektaş and Çapkınoğlu Bektaş and Çapkinoğlu 1997). The southern margin of the Black Sea has been determined to thrust along the Georgia to Romanian belt (Barka and Reilinger 1997). This thrust belt is intersected by strike-slip faults such as the Rize fault, the Trabzon fault, and the Ordu fault (Bektaş et al. 1995).

An 815-km-long highway was recently built on the Black Sea coast, between Samsun and Sarp. Filling material was used to push back the Black Sea during the construction of this highway (Kaya et al. 2003). A large number of blasts have been detonated in different surface quarries to produce the filling material over the course of nearly two decades. These quarry blasts have been recorded by the regional seismic network and represent the dataset for the current study. The seismic recorders not only record the earthquakes occurring in the area but also quarry, mine, and chemical blasting and other artificial sources. These artificial events contaminate the seismicity catalogs, causing seismic risk and hazard studies in the region to be assessed incorrectly. Since it is necessary to use a uniform earthquake catalog in these studies, artificial events such as quarry blasts should be excluded from regional catalogs. Discrimination of earthquakes from quarry blasts using simple methods, i.e., satellite images, occurrence times, may not be accurate if quarries are located along active fault zones (Horasan et al. 2009; Wiemer and Baer 2000). Discrimination can be made by applying different methods to both the time and frequency domain. Wüster (1993) used Lg/Pg and Lg/
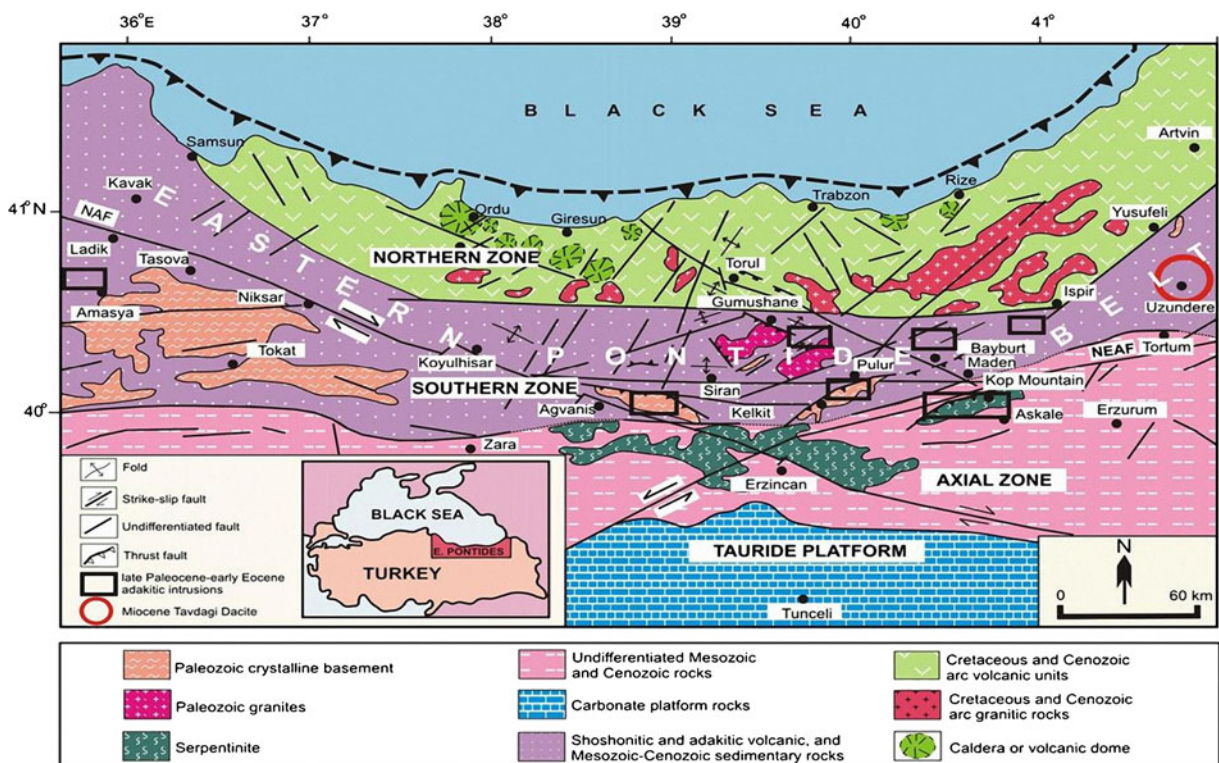
Fig. 1 Generalized tectonic map showing main zones and lithological units of the eastern Pontides orogenic belt. *NAF* North Anatolian Fault, *NEAF* North East Anatolian Fault (Eyüboglu et al. 2012). *Green*, *purple*, and *pink areas* represent in northern zone, southern zone, and axial zone, respectively

Rg ratio methods in Germany/Czechoslovakia. Baumgardt and Young (1990) considered the ratios of Pn/Sn and Pn/Lg for Western Norway. Gitterman and Shapira (1993) used the spectral rate of low and high frequencies of seismic energy. Seismic events were examined in the domains of time and frequency by Horasan et al. (2009) for Istanbul and vicinity, Sertçelik and Başer (2010) for the South Aegean Region, Öğütçü et al. (2011) for Konya and its vicinity, and Kartal and Horasan (2011) for Trabzon and its vicinity. Kekovali et al. (2011) estimated capability of potential mining and quarry areas from seismic catalog using statistical analysis for Turkey.

The purpose of this study is to discriminate surface quarry blasts from earthquakes in seismic events recorded between 2002 and 2010 in the eastern Black Sea area (lon 37.6° E–42.0° E and lat 40.2–41.5° N). These events were recorded by the Trabzon (KTUT), Espiye (ESPY), Gümüşhane (GUMT), Aydıntepe (BAYT), Borçka (BCA), and Pazar (PZAR) stations belonging to Karadeniz Technical University (KTU) and the Bogaziçi University Kandilli Observatory Earthquake Research Institute (KOERI). After eliminating quarry blasts, we will have a catalog that contains only the earthquakes that occurred in this region, thus identifying the seismicity level of the eastern Black Sea region and its active faults generating earthquakes. Furthermore, future seismic risk and hazard studies made using this catalog will yield more accurate results.

2 Data and methods

In this study, we examined 186 seismic events by KTU and KOERI stations between the years of 2002 and 2010. An overview of the stations is listed in Table 1. Stations KTUT, ESPY, PZAR, BCA, and BAYT are equipped with broad-band seismometers and GUMT with a short period sensor. Figure 2 shows the epicenter distribution of the all seismic events recorded, seismic stations and quarries in the region between 2002 and 2010. The magnitudes, locations, and depths of the events are taken from Seismological Observatory of KOERI that provides and the real-time data with the modern on-line and dial-up seismic stations in Turkey and determines, as rapidly and accurately as possible, the location and magnitude of all earthquakes. Generally, the duration magnitudes

Table 1 General information about the stations used in the study

Station	Latitude	Longitude	Station type
KTUT	40.9870	39.7667	Broad Band
ESPY	40.9167	38.7273	Broad Band
PZAR	41.1780	40.8988	Broad Band
BAYT	40.3935	40.1410	Broad Band
BCA	41.4450	41.6223	Broad Band
GUMT	40.4675	39.4780	Short Period

(Md) of the events range between 2 and 3.5. Only two seismic events with $M>4.0$ have been recorded in the period from 2002–2010. The first event (Md= 4.2, 20 Jun 2008) occurred on the Eynesil–Giresun coast and the second event (Md=4.6, 18 Nov 2003) occurred in Artvin. The focal depths all the events in the region ranged between 2.1 and 26.5 km. Between 2006 and 2010, the maximal localization errors (ERH) amounted to 5 and 10 km for the on- and off-shore seismicity, respectively. The corresponding RMS error values are 0.1–0.5 s and 0.3–0.8 s.

The daytime distributions of seismic events in the studied area are shown in Fig. 3, demonstrating that seismic activity is highest between 10 a.m. and 2 p.m. GMT (12 a.m. and 4 p.m. local time).

We have identified two steps in this study. As a first step, to determine dataset we used simple criteria that belong to distinguish earthquakes from quarry blasts. These basic criteria were separation of daytime and nighttime, epicenter distance, magnitude, and focal depth. Earthquakes can occur at any hours during the day. However quarry blasts commonly occur during the working hours (8 a.m. and 5 p.m. local time) of the day (Horasan et al. 2009; Wiemer and Baer 2000). Additionally, quarry blasts occur on land and near the surface. Another case, commonly quarry blasts have magnitudes and focal depths smaller than about 3.0 and 10 km, respectively. Therefore, we selected 186 seismic events from recorded 319 events between 2002 and 2010 that occurred on land, hours of the working days, smaller than 3.0 magnitudes, and 15 km focal depth. We considered the events occurred in the Black Sea, occurred during the nighttime on land, greater than magnitude, and focal depth 3.0 and 10 km as earthquakes. Thus, we examined the 186 events which are marked by purple hexagon in Fig. 2 occurred on the land during the daytime. In the second
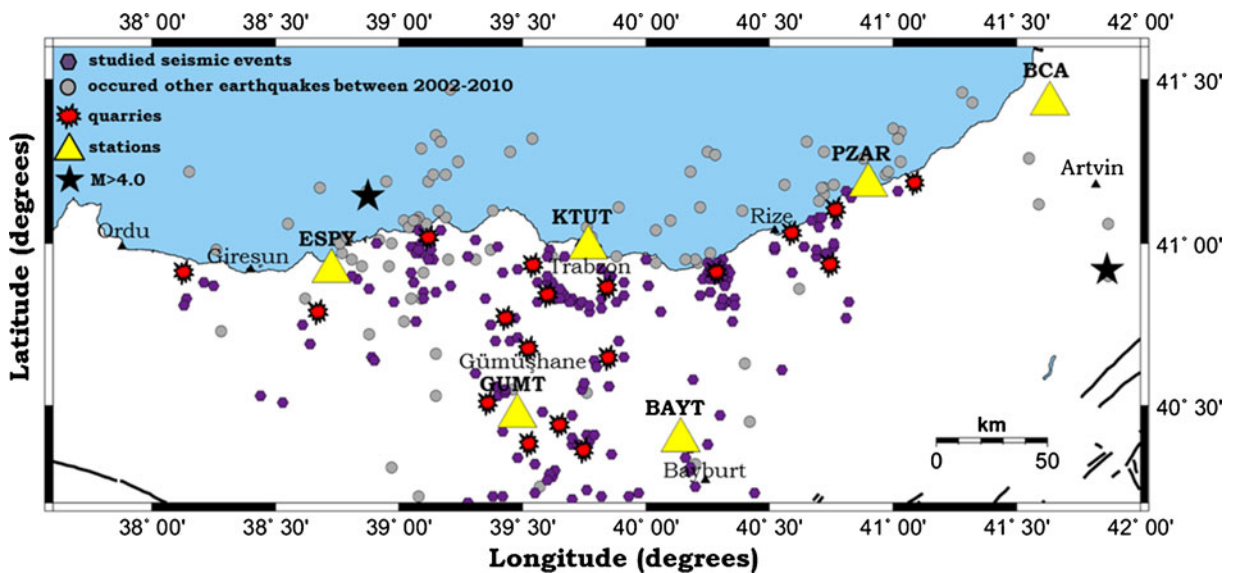
Fig. 2 Map of the distribution of seismic stations, major quarries, and seismic events between 2002 to 2010 in the study area (*purple hexagons* show studied seismic events, *gray circles* show earthquake occurred during nighttime and also in the Black Sea, *red symbols* show quarries, and *yellow triangles* show seismic stations of KTUT, ESPY, PZAR, BCA, BAYT, and GUMT)

step, we analyzed statistical and spectral new dataset in detail. In order to distinguish these events, we used three different methods, considering the S/P to logS amplitude ratio, the discrimination of complexity and spectral ratios, and two dimensional time-frequency analysis (TFA).

The first method used in the analysis plots the amplitude peak ratio of the S to P waves versus the logarithm amplitude peak of the S wave in the time domain of the seismogram (Wüster 1993; Baumgardt and Young 1990). For each of the 186 seismic events, the maximum
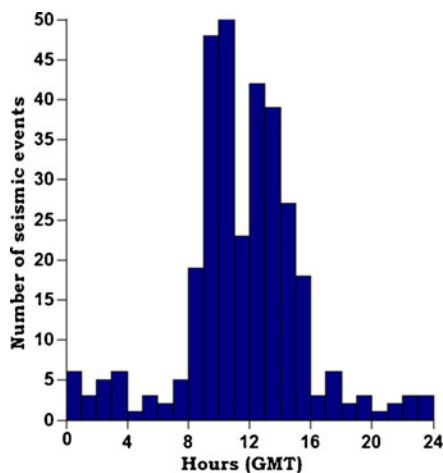
Fig. 3 Distribution of the seismic events by time of day in the study area

of P and S wave amplitudes were read from the vertical component records of stations KTUT, ESPY, BAYT, BCA, PZAR, and GUMT. The ratio of maximum S wave amplitude to the maximum P wave amplitude (S/ P) was drawn against the logarithm of maximum S wave amplitudes (logS). Then, linear discriminant function (LDF) analysis was used to distinguish earthquakes from quarry blasts (Fisher 1936).

LDF is related to both multivariate analysis of variance and multiple regressions and is used to determine the variables that discriminate between two or more naturally-occurring groups. In the two-group case, discriminant function analysis can also be thought of as a multiple regression process. If the two groups from analyses 1 and 2 used that variable as the dependent variable in a multiple regression analysis, then they would yield results that are analogous to those that would be obtained via discriminant analysis (Hill and Lewicki 2007).

In general, two-group linear discriminant functions can be demonstrated simply, as below:

$$group = a + b_1x_1 + b_2x_{2\ldots} + b_mx_m \qquad (1)$$

where a is a constant, b_1 through b_m are regression coefficients, and x_1 is the standardized value of x_m discriminating variables. The interpretation of the results of a two-group problem is straightforward and closely follows the logic of multiple regressions. Those variables with the largest regression coefficients are the

ones that contribute most to the prediction of group membership (Hill and Lewicki 2007). A MATLAB program was developed for LDF analysis using algorithms given by Vojtech and Hlavac (2004). The ratio of S/P to logS was calculated separately for each station.

In the discriminant analysis between earthquakes and quarry blast, a second method was employed plotting complexity (C) versus the spectral ratio of the seismogram (Sr). In these definitions, C is the ratio of the seismogram's integrated powers s^2 (t) in the selected time windows (t_1–t_2 and t_0–t_1). Sr is the ratio of the seismogram's integrated spectral amplitudes $a(f)$ in the selected frequency bands (high-frequency band, h_1–h_2, and low-frequency band, l_1–l_2). C and Sr can be written as below (Arai and Yosida 2004; Gitterman and Shapira 1993):

$$C = \int_{t1}^{t2} S^2(t)\mathrm{dt} \Big/ \int_{t0}^{t1} S^2(t)\mathrm{dt} \tag{2}$$

$$Sr = \int_{h1}^{h2} a(f)\mathrm{df} \Big/ \int_{l1}^{l2} a(f)\mathrm{df} \tag{3}$$

The limits of the integrals (t_0, t_1, and t_2) of C given in Eq. (2) were determined by a trial-and-error approach to find the best representative C values for both blasts and earthquakes having the same magnitude. For example, C values of blasts and earthquakes are 0.59 and 11 for selected time windows of t_0=0 s, t_1= 2 s, and t_2=4 s. The C value of blasts increases as the selected length of the time window increases (C=0.59 for t_0=0 s, t_1=2 s, and t_2=4 s; C=0.62 for t_0=0 s, t_1= 2 s, and t_2=5 s) (Horasan et al. 2009). For this reason, the greatest available time window was chosen in distinguishing blasts from earthquakes based on the calculated C values. The limits of the integrals (h_1, h_2, l_1, and l_2) used in the calculation of spectral amplitudes for Sr in Eq. (3) were determined by comparing the spectra of quarry blasts with those of earthquakes (Horasan et al. 2009).

The P wave energy of a quarry blast is greater than that of the S wave, whereas the S wave energy of earthquakes is larger than that of the P wave. The frequencies and phases of the seismic waves resulting from earthquakes and explosions are different. Earthquakes have a wider bandwidth, than quarry blast. P waves resulting

from explosions contain higher frequencies and more impulses. Fourier analysis converts a signal from the time domain to the frequency domain. However, this method does not give information about the frequency values, which correspond to the time periods. The TFA method transforms a one-dimensional (1-D) signal into a two-dimensional (2-D) function of time and frequency and illustrates how the spectral content of the signal changes with time. TFA indicate changes in signal frequency content over time by combining time-frequency functions (Cohen 1989). Using TFA with seismic records, it is easier to identify possible small blasts. In this study, we used a short-time Fourier transform (STFT), which is a linear TFA.

The basic concept in the STFT method is to divide the signal into small segments of the same width and perform Fourier analysis on each of them to determine the frequencies present in each segment (Cohen 1995). The amplitude distribution is defined in Eq. (4) by STFT through the linear integral,

$$\mathrm{STFT}_x(t,f) = \int_{-\infty}^{\infty} x(\tau).h(\tau - t).e^{-i2\pi f\tau}\mathrm{dt} \tag{4}$$

The STFT method (Gabor 1946) shows the local spectrum of signal $x(\tau)$ around time t, selected by localization window $h(t)$. A MATLAB program was used for STFT analysis using algorithms given by Auger et al. (1997).

3 Results and discussion

The maximum epicenter distance between events and stations used in this study, is about 200 km. Because the Moho depth changes about 40 km (Grad et al. 2009) in this study area and consequently the cross over distance about 200–210 km. Since this value is lower than the cross-over distance in this region, we considered all first arrival as Pg phase. The ratios of S/P to logS values were calculated and plotted for each station. Figure 4 shows the amplitude peak ratios of S to P waves versus the logarithms of amplitude peaks of S waves in the time domain for the vertical components of the seismograms of the investigated seismic events recorded by the KTUT, ESPY, BAYT, PZAR, GUMT, and BCA stations, respectively. In order to apply the LDF method to the seismic events, we divided the ratios of S/P into
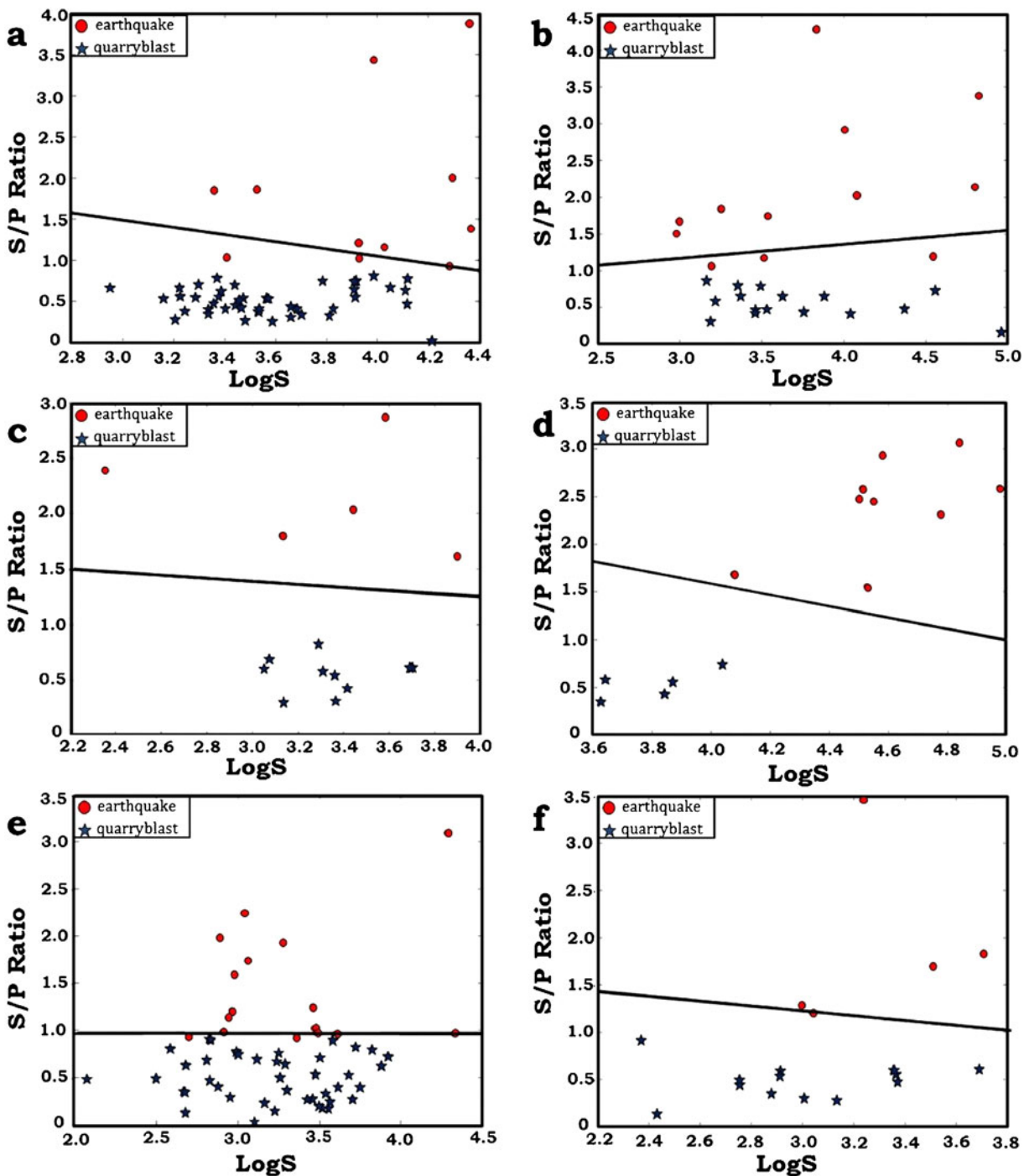
Fig. 4 Graphics of S/P versus logS determined from the records in time domain of the vertical component of the seismograms stations: KTUT (**a**), ESPY (**b**), BAYT (**c**), PZAR (**d**), GUMT (**e**), and BCA (**f**). The discrimination line has been determined from a LDF for each station (*blue stars* show quarry blast and *red circles* show earthquakes)

two different groups, because the S amplitudes of earthquakes are larger and the P amplitudes lower than those of blasts. The first group, likely blasts, includes

amplitude ratios lower than 1.0 and the second group, likely earthquakes, includes those greater than 1.0. The lines separating earthquakes from quarry blasts (Fig. 4;

Table 2) were determined through LDF using algorithms given by Vojtech and Hlavac (2004). Blue stars in Fig. 4 are quarry blasts, and red circles are earthquakes. According to this distinction, accuracy classifications are 96.3, 89.3, 100, 100, 96.5, and 100 % for stations KTUT, ESPY, BAYT, PZAR, GUMT, and BCA, respectively.

The results from the LDF analysis showed, that in some cases this method could not separate earthquakes and quarry blasts. Some earthquakes remained below the lines of discrimination (Fig. 4a, b, e). The criteria used in this study for LDF analysis were that S/P be lower than 1.0 for the blast group and S/P be higher than 1.0 for the earthquake group. As seen in Fig. 4, if the S/P ratio is around 1.0, earthquakes are placed under the discrimination lines and interpreted as blasts. In these cases, we used Fourier transforms and TFA to decide whether these events were earthquakes or blasts.

C–Sr ratio values were calculated and plotted for each station. Figure 5 shows complexity (C) versus the spectral ratio (Sr) for the investigated seismic events in stations KTUT, ESPY, BAYT, PZAR, GUMT, and BCA, respectively. The time windows and frequency bands used in the calculation of C and Sr were selected as t_1–t_2 (3–10 s) and t_0–t_1 (the onset time of the P wave —3 s) and h_1–h_2 (8–15 Hz) and l_1–l_2 (1–7 Hz), respectively; C becomes larger for earthquakes in comparison with quarry blasts. According to this method, correct classifications occurred in 94.4, 85.7, 100, 73.3, 91.2, and 78 % of the cases for stations KTUT, ESPY, BAYT, PZAR, GUMT, and BCA, respectively.

Table 2 The results of discriminant analysis of methods of the S/P versus logS between earthquake and quarry blasts for BAYT, KTUT, BCA, ESPY, PZAR and GUMT stations

Station	Type	Predicted type		Total
		Blast	Earthquake	
BAYT	Original	Blast	10	0	10
		Earthquake	0	5	5
	%	Blast	100	0	100
		Earthquake	0	100	100
KTUT	Original	Blast	44	0	44
		Earthquake	2	8	10
	%	Blast	100	0	100
		Earthquake	20	80	100
BCA	Original	Blast	13	0	13
		Earthquake	0	5	5
	%	Blast	100	0	100
		Earthquake	0	100	100
ESPY	Original	Blast	16	0	16
		Earthquake	3	9	12
	%	Blast	100	0	100
		Earthquake	25	75	100
PZAR	Original	Blast	5	0	5
		Earthquake	0	9	9
	%	Blast	100	0	100
		Earthquake	0	100	100
GUMT	Original	Blast	41	0	41
		Earthquake	2	14	16
	%	Blast	100	0	100
		Earthquake	12.5	87.5	100
Total events		Blast	129	0	129
		Earthquake	7	50	57

The percentages of classifications are 96.3, 89.3, 100, 100, 100, and 96.5 % for stations KTUT, ESPY, BAYT, PZAR, BCA, and GUMT, respectively
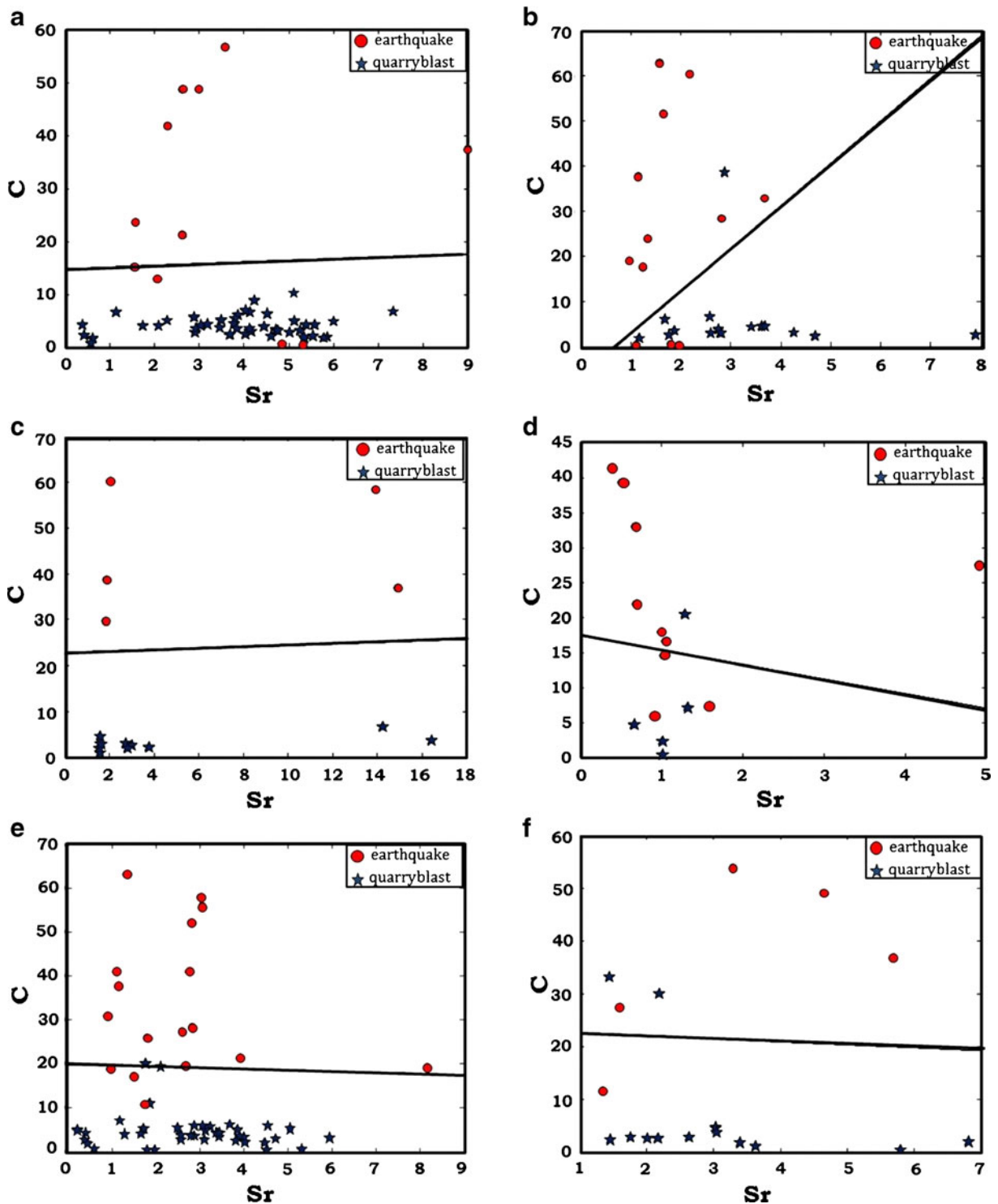
Fig. 5 Distribution of complexity-spectral ratio (*C-Sr*) of the seismograms stations: KTUT (**a**), ESPY (**b**), BAYT (**c**), PZAR (**d**), GUMT (**e**), and BCA (**f**). The discrimination line has been determined from a LDF for each station (*blue stars* show quarry blast and *red circles* show earthquakes)

The results of the classification ratios observed using the two methods indicate that the S/P versus logS method provides better discrimination between earthquakes and quarry blasts than the C–Sr method.

We applied Fourier transforms and TFA to the events, formerly not explicitly discriminated. Statistical methods may give incorrect results in some cases, such as inaccurate identification of the wave amplitudes on the seismograms, or errors in the calculations of the values related to time and frequency intervals. Hence, the records of the remaining events need to be further examined by spectral methods. Generally, to examine the frequency of the seismograms, a 1-D Fourier transform has been used in the literature. For example, Horasan et al. (2009), Öğütçü et al. (2011), and Kartal and Horasan (2011) used spectral analysis with a Fourier transform. However in recent years TFA method has been used in the analysis of seismic events records and the discrimination of earthquakes and explosions (Arrowsmith 2009; Kristekova et al. 2008). As well as using the 1-D Fourier method, we used the TFA for the first time in Turkey in this study to distinguish earthquake and explosion records.

We considered two criteria to separate earthquakes and explosions in the TFA method: the distributions of maximum wave amplitudes and different phase groups. The first criterion is to observe the maximum released energy. For quarry blasts, energy is released suddenly and maximum amplitudes are observed in the beginning of the record in the time. The maximum energy spreads through large frequencies in the frequency domain and is concentrated in the first part of the TFA. In earthquake records, S wave amplitudes are much larger than P wave amplitudes. Maximum amplitudes are observed in the S wave train arriving later than the P wave train in the time domain. The maximum energy spreads through lower frequencies than those of P waves in the frequency domain and is not concentrated in the first part of the TFA. The second criterion of discrimination is the observation of the Rg phase. The Rg phase, often observed on the vertical component records of quarry blasts and very shallowly focused earthquakes, has a spectral peak at 0.5–2.0 Hz (Kim et al. 1994). Quarry blasts often consist of several delayed blasts for economic and safety reasons. This is called ripple firing or delayed shooting. The multiple explosions modulate the spectrum of the signal. Hedlin et al. (1989,

Fig. 6 The vertical component of the seismograms in the time, frequency and time-frequency domain with STFT. Spectrogram of the Trabzon Hayrat quarry blast (Md=2.7) recorded at station BAYT on 20 Oct 2008. The Rg phase can be observed at 12 s/4 Hz
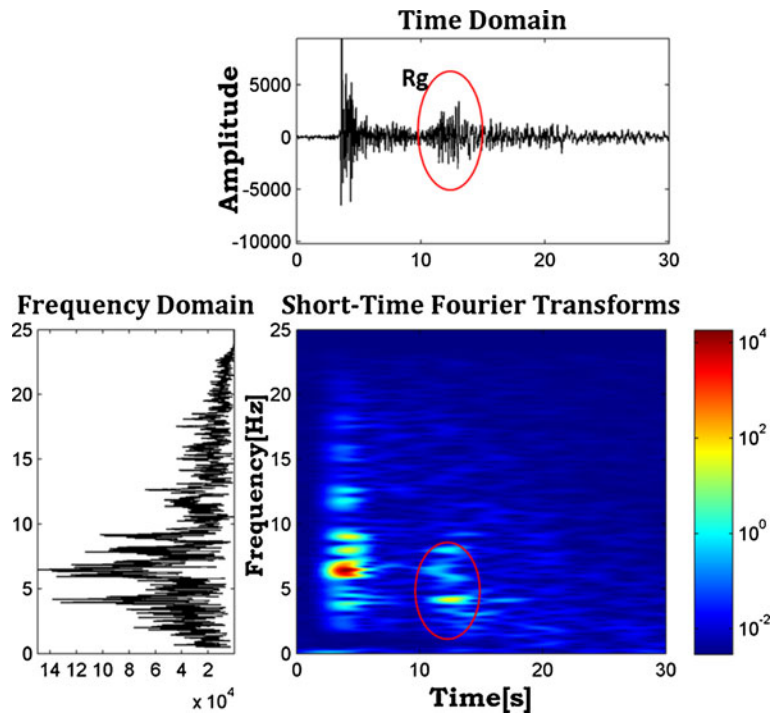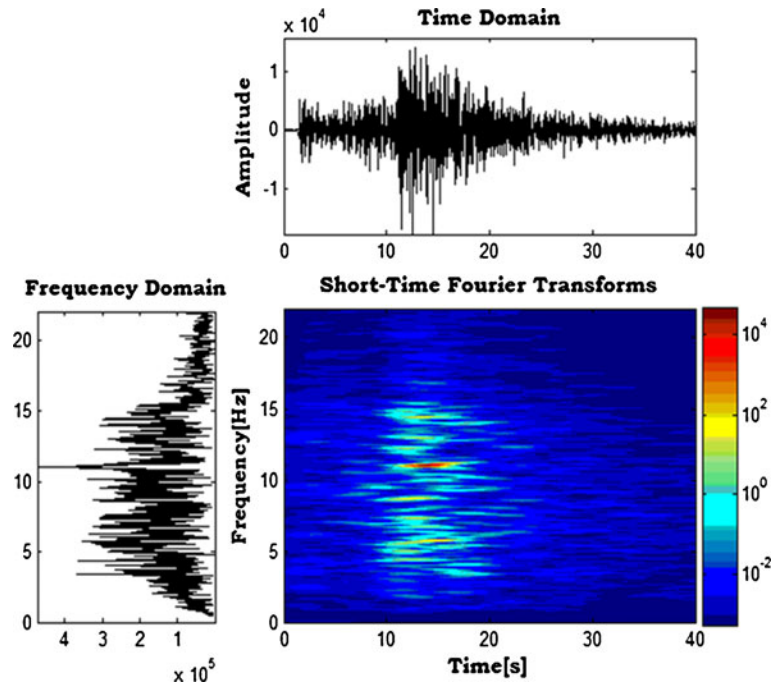
Fig. 7 The vertical component of the seismograms in the time, frequency, and time-frequency domain with STFT. Spectrogram of the Giresun–Görele quarry blast (Md=2.6) recorded at station GUMT on 27 Jan 2008
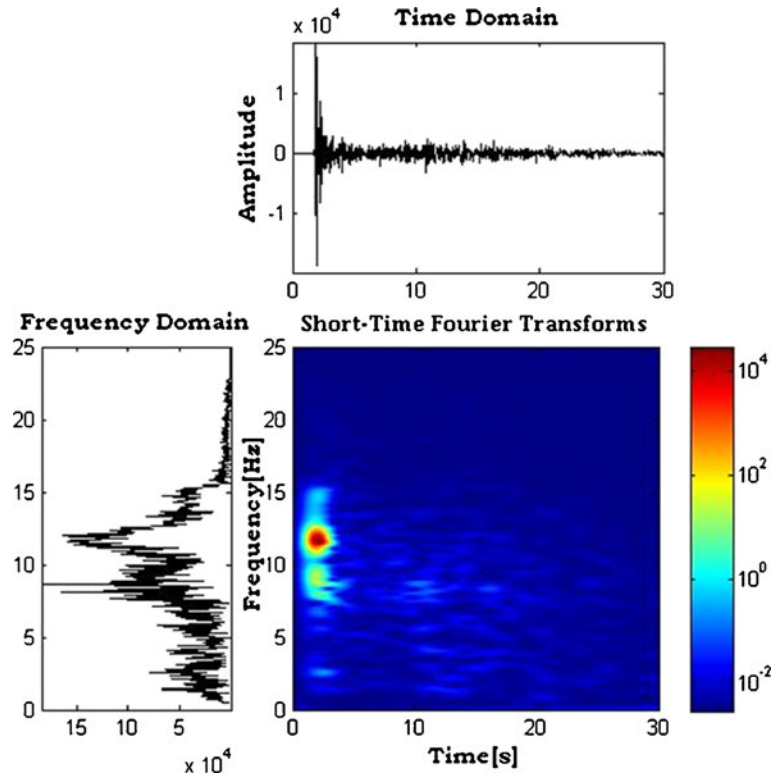
1990) and Beck and Wallace (1995) used this property to discriminate between ripple-fired blasts and earthquakes.

Figures 6, 7, 8, and 9 show the vertical components of the time domain, frequency domain, and 2-D TFA with STFT method for a quarry blasts and earthquakes,

Fig. 8 The vertical component of the seismograms in the time, frequency and time-frequency domain with STFT. Spectrogram of the Trabzon earthquake (Md=2.9) recorded at station GUMT on 17 Feb 2008

Fig. 9 The vertical component of the seismograms in the time, frequency and time-frequency domain with STFT. Spectrogram of the Giresun–Eynesil earthquake (Md=2.9) recorded at station KTUT on 23 Jan 2007
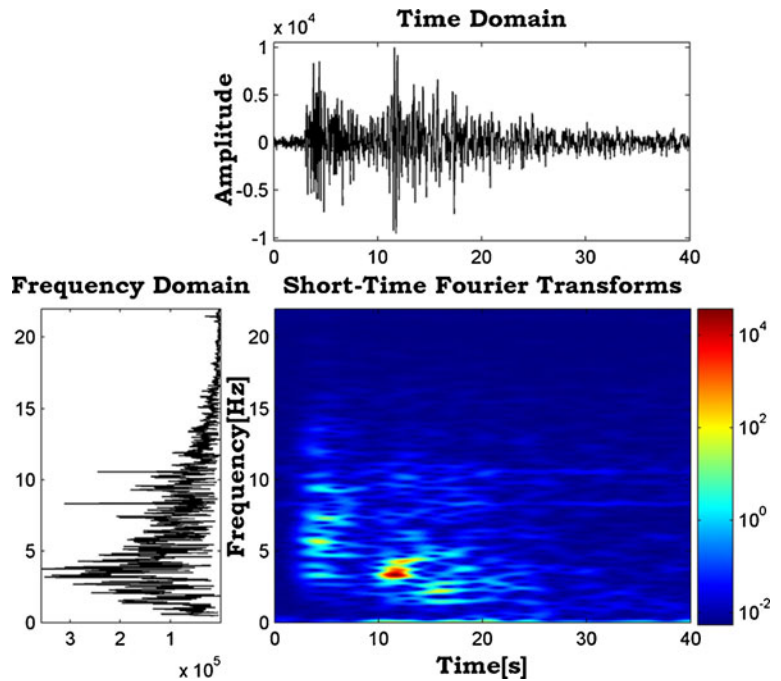
respectively. Figures 6 and 7 show P wave amplitudes are much greater than those of other phases. The maximum energy, shown in red, is released around 4 s in the time domain and 6.5 Hz in the frequency domain in Fig. 6. The Rg phase, represented in yellow, can be seen between 10 and 15 s in the time domain and between 3 and 4 Hz in the frequency domain in Fig. 6. Figure 7 shows the maximum energy released around 2 s in the time domain and 12 Hz in the frequency domain. Figures 8 and 9 show amplitudes of S waves are much larger than those of P waves, and the maximum energy is released between 10 and 15 s in the time domain. Considering the abovementioned criteria related to the released maximum energy and Rg phase, we have decided that the event in Figs. 6 and 7 are quarry blasts and Figs. 8 and 9 are earthquakes.
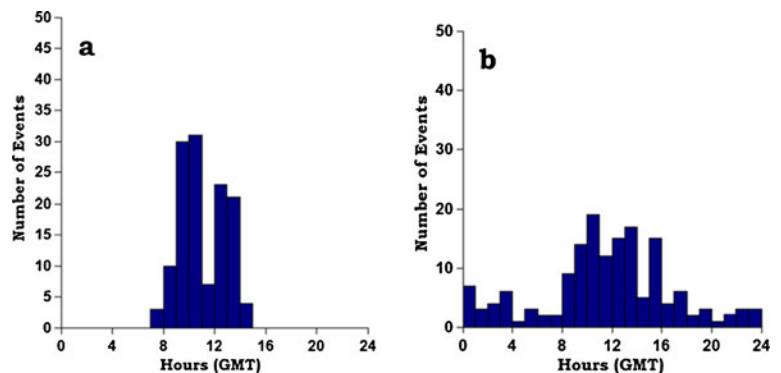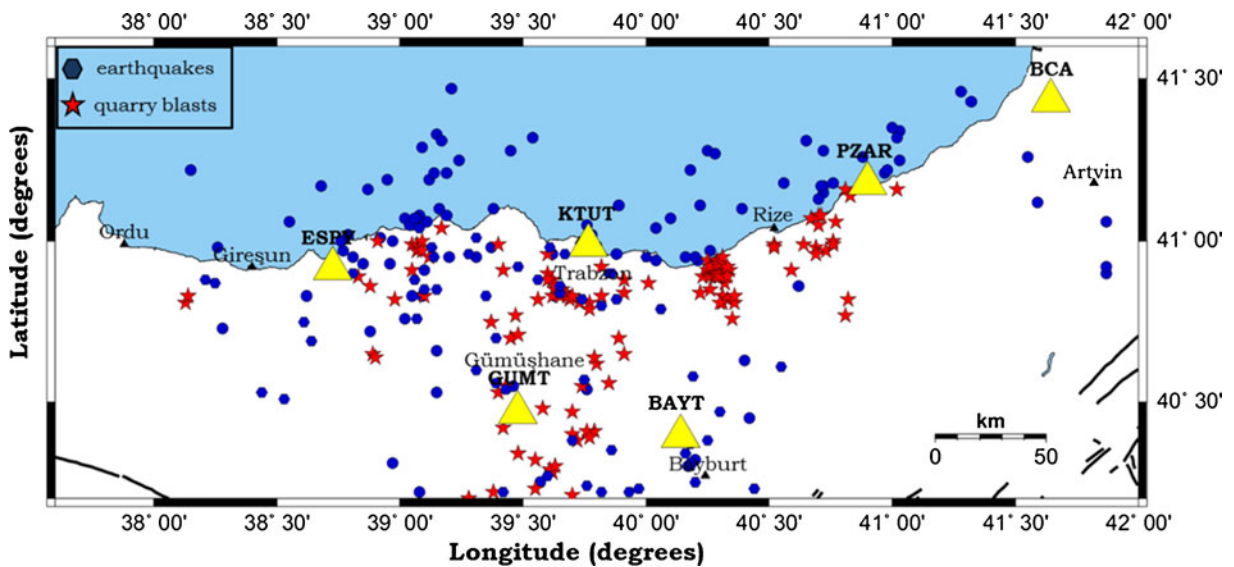
Figure 10a, b shows the distribution of the number of quarry blasts versus time in the region and earthquakes versus time in the region after removing quarry blasts, respectively. Comparing Figs. 3 and 10b shows clearly that the methods applied to remove blasts have greatly reduced the number of events during the daytime. While quarry blasts occur during the daytime, earthquakes occur at any time of the day. However, the number of earthquakes observed during the daytime is slightly higher than the number of earthquakes occurring at night. Some of the earthquakes examined in this study were observed in the daytime. For example, the earthquakes on the coast of Giresun, (31 July 2005, Md=3.4, at 09:17), at Trabzon (16 March 2006, Md=3.1, at 12:05), and on the coast of Eynesil (20 September 2006, Md=3.5, at 09:26) and the coast

Fig. 10 Histogram of daytime occurrence after the application of the discrimination criteria: (a) for quarry blast and (b) for earthquake recorded in the study area

Fig. 11 Epicenter map after the application of the discrimination criteria: quarry blasts (*red stars*), earthquakes (*blue hexagons*), and seismic stations (*yellow triangles*)

of Espiye (20 June 2008, Md=4.2, at 08:23) occurred during the daytime.

The locations of both earthquakes and quarry blasts in this study are mapped in Fig. 11 (red stars are quarry blast and blue hexagons are earthquakes). A large part of earthquakes and quarry blasts shown on this map are separated using the statistical S/P–logS and C–Sr methods. In addition, the TFA method is used to define events not separated statistically. As a result of these methods, we detected 128 quarry blasts and 58 earthquakes from 186 seismic events, which show that 32 % of the investigated seismic events are earthquakes and 68 % are quarry blasts. We have given in as a scheme that according to the simple discriminant criteria and analysis criteria, the remaining number of quarry blasts and earthquakes in Table 3. Considering all the events between the years of 2002 and 2010 show that 59.87 % are earthquake and 40.13 % are quarry blasts.

The earthquakes occurring on land are related to small faults such as the Bayburt–Gümüşhane–Espiye and Alucra–Torul–Trabzon faults (Bektaş and Çapkınoğlu 1997). The blasts are concentrated in the large quarries (for example, the Of, Maçka, Görele, and Rize quarries). Nearly 40 % of the earthquakes occurred in the Black Sea, most of them are related to the Black Sea thrust belt. The largest earthquake observed between 2002 and 2010 in the Black Sea was the 2008 Eynesil earthquake (Md= 4.2), which occurred on this belt. Two large earthquakes

in the last century, the 1959 Batum earthquake (M=6.2) and the 1968 Bartın earthquake (M=6.8), were related to the Black Sea thrust belt (Barka and Reilinger 1997). It can be concluded that the sea holds the greatest earthquake potential in the eastern Black Sea region.

4 Conclusions

We analyzed seismic events recorded between 2002 and 2010 to discriminate quarry blasts from earthquakes in

Table 3 The remaining number of quarry blasts and earthquakes according to the simple discriminant criteria and analysis criteria of earthquakes

Simple discriminant criteria	Number of events
Initial number of events	319
Off-shore	−58
Day/night	−39
Depth	−23
Magnitude	−13
Analysis criteria	186
S/P–logS ratio	−50
C–Sr ratio	−46
TFA	−32
Remaining	128 quarry blast=68 %
	58 earthquake=32 %

the eastern Black Sea region. We applied the methods of S/P to logS amplitude ratio, discriminating by complexity and spectral ratio, and 2-D TFA. The 186 of originally 319 recorded seismic events in the region by stations KTUT, ESPY, BAYT, PZAR, BCA, and GUMT were examined.

After applying all methods, we detected 128 quarry blasts and 58 earthquakes. This shows that 32 % of the investigated seismic events were earthquakes and 68 % were quarry blasts. However considering all the events between the years of 2002 and 2010 show that 59.87 % are earthquake and 40.13 % are quarry blasts. The blasts were made during the daytime and concentrated in the large quarries such as Of, Maçka, and Görele. About 60 % of the earthquakes occurred on land and were related to faults that generally generate earthquakes smaller than 3.5. The earthquakes that occurred in the Black Sea are related to the Black Sea thrust belt, where two large earthquakes have been observed in the last century. The largest observed earthquake in the Black Sea during the period studied was the 2008 Eynesil earthquake (Md=4.2). We conclude that in the examined area, earthquakes are more likely to be generated in the Black Sea than on land.

References

Auger F, Flandrin P, Goncalves P, Lemoine O (1997) Time-Frequency Toolbox for Use with Matlab: reference Guide. CNRS, France

Arai N, Yosida Y (2004) Discrimination by short-period seismograms. International Institute of Seismology and Earthquake Engineering, Building Research Institute (IISEE). Lecture Note, Global Course, Tsukuba, Japan, p. 10

Arrowsmith MD (2009) Mining explosion identification as an application to treaty verification. Ph.D. dissertation, Southern Methodist University, p. 519

Baumgardt DR, Young GB (1990) Regional seismic waveform discriminates and case-based event identification using regional arrays. Bull Seism Soc Am 80:1874–1892

Barka A, Reilinger R (1997) Active Tectonics of Eastern Mediterranean region: deduced from GPS, neotectonic and seismicity data. Ann Geofis X2:587–610

Beck SL, Wallace TC (1995) Broadband seismic recordings of mining explosions and earthquakes in South America. In: 17th Seismic Research Symposium on Monitoring a CTBT Scottsdale, pp. 157–163

Bektaş O, Yilmaz C, Tasli K, Akdağ K, Özgür S (1995) Cretaceous rifting of the eastern Pontide carbonate platform (NE Turkey): the formation of carbonates breccias and turbidites as evidences of a drowned platform. Geologia 57:233–244

Bektaş O, Çapkinoğlu Ş (1997) Neptunian dikes and block tectonis in the eastern pontide magmatic are, NE Turkey: implications for the kinematics of the mesozoic basins. Geosound 30:451–461

Chekunov AV, Pustovitenko BG, Kulchitskiy VE (1994) Seismicity and deep tectonics of the Black Sea depression and its margins. Geotectonics 28:221–225

Cohen L (1989) Time-frequency distributions: a review. Proceedings of the Institute of Electrical and Electronics Engineers (IEEE) 77:941–981

Cohen L (1995) Time-frequency signal analysis. Prentice-Hall, New York

Eyüboğlu Y, Bektaş O, Pul D (2007) Mid-cretaceous olistostromal ophiolitic melange developed in the back-arc basin of the eastern pontide magmatic arc (NE Turkey). Int Geol Rev 49:1103–1126

Eyüboğlu Y, Santosh M, Yi K, Bektaş O, Kwon S (2012) Discovery of Miocene adakitic dacite from the Eastern Pontides Belt and revised geodynamic model for the late Cenozoic evolution of eastern Mediterranean region. Lithos 146–147:218–232

Fisher RA (1936) The use of multiple measurements in taxonomic problems. Annals of Eugenics 7:179–188

Gabor D (1946) Theory of communication. Journal of the Institution of Electrical Engineers (IEE) 3:429–457

Gitterman Y, Shapira A (1993) Spectral discrimination of underwater explosions. Isr J Earth Sci 42:37–44

Grad M, Tiira T, ESC Working Group (2009) The Moho depth map of the European Plate. Geophys J Int 176:279–292

Hedlin MA, Minster JB, Orcutt JA (1989) The time-frequency characteristics of quarry blasts and calibration explosions recorded in Kazakstan, USSR. Geophys J 99:109–121

Hedlin M, Minster JB, Orcutt JA (1990) An automatic means to discriminate between earthquakes and quarry blasts. Bull Seism Soc Am 80:2143–2160

Hill T, Lewicki P (2007) Statistics: methods and applications. StatSoft, Tulsa, OK

Horasan G, Boztepe-Güney A, Küsmezer A, Bekler F, Öğütçü Z, Musaoğlu N (2009) Contamination of seismicity catalogs by quarry basts: an example from Istanbul and its vicinity, northwestern Turkey. J Asian Earth Sci 34:90–99

Kartal ÖF, Horasan G (2011) Trabzon ve civarındaki deprem ve patlatma verilerinin birbirinden ayırt edilmesi (Discrimination of quarry blasts and earthquakes in Trabzon and its vicinity). SAÜ Fen Bilimleri Dergisi 15:68–74

Kaya R, Kesimal A, Yılmaz E, Erçıktı B (2003) Karadeniz Sahil Yolu Projesi Kapsamında Trabzonda İşletilen Taş Ocaklarında Yapılan Patlatmaların Çevresel Açıdan İncelenmesi. 3. Kırmataş Sempozyumu İstanbul., pp 91–97

Kekovali K, Kalafat D, Kara M, Deniz P (2011) The estimation capability of potential mining and quarry areas from seismic catalog using statistical analysis, an application to Turkey. Int J Phys Sci 6:3784–3794

Kim WY, Simpson DW, Richards PG (1994) High-frequency spectra of regional phases from earthquakes and chemical explosions. Bull Seism Soc Am 84:1365–1386

Kristekova M, Moczo P, Labak P, Cipciar A, Fojtikova L, Madaras J, Kristek J (2008) Time-frequency analysis of explosions in the ammunition factory in Novaky, Slovakia. Bull Seism Soc Am 98:2507–2516

Öğütçü Z, Horasan G, Kalafat D (2011) Investigation of micro seismic activity sources in Konya and its vicinity, Central Turkey. Nat Hazards 58:497–509

Sertçelik F, Başer O (2010) Güney Ege Bölgesi'nde yapay ve doğal kaynaklı titreşimlerin ayırt edilmesi (Discrimination of artificial and natural sourced vibrations in the southern Aegean Region). Yerbilimleri 31:233–245

Vojtech F, Hlavac V (2004) Statistical pattern recognition toolbox for MATLAB (SPRTOOL). User's guide. Available from http://cmp.felk.cvut.cz/cmp/cmp_software.htlm

Wessel P, Smith WHF (1995) New version of the generic mapping tools (GMT) version 3.0 released. Transactions American Geophysical Union 76:32

Wiemer S, Baer M (2000) Mapping and removing quarry blast events from seismicity catalogs, short notes. Bull Seism Soc Am 90:525–530

Wüster J (1993) Discrimination of chemical explosions and earthquakes in central Europa—a case study. Bull Seism Soc Am 83:184–1212